https://ntrs.nasa.gov/search.jsp?R=19930083675 2020-06-17T20:31:08+00:00Z

CASE FILE COPY

Copy # 2

NACA TN 3038

NATIONAL ADVISORY COMMITTEE FOR AERONAUTICS

TECHNICAL NOTE 3038

LOW-SPEED DRAG OF CYLINDERS OF VARIOUS SHAPES

By Noel K. Delany and Norman E. Sorensen

Ames Aeronautical Laboratory
Moffett Field, Calif.

MAY 22 1956

Washington
November 1953

PROPERTY FAIRCHILD ENGINEERING LIBRARY

NATIONAL ADVISORY COMMITTEE FOR AERONAUTICS

TECHNICAL NOTE 3038

LOW-SPEED DRAG OF CYLINDERS OF VARIOUS SHAPES

By Noel K. Delany and Norman E. Sorensen

SUMMARY

An investigation has been conducted to find the approximate variation of the drag coefficient with Reynolds number of several cylinders having different cross-sectional shapes. Data were obtained for circular cylinders, elliptical cylinders of two fineness ratios, rectangular and diamond cylinders of three fineness ratios, and two isosceles triangular cylinders (apex forward and base forward). Three different corner radii were tested on each of the shapes, except for the circular and elliptical cylinders. Data were obtained for Reynolds numbers as low as 11,000 and as high as 2,300,000. For some cylinders, frequencies of pressure fluctuations in the wake were measured for a limited range of Reynolds numbers.

INTRODUCTION

A method of estimating the effects of viscosity on the forces and moments for inclined bodies has recently been suggested (e.g., see refs. 1 and 2). In the proposed method, the crossflow in planes perpendicular to the inclined axis of the body has been related to the flow around a cylinder, and, hence, the resulting cross forces are related to the section drag coefficient. The use of the method requires a knowledge of the section drag characteristics of cylinders. For bodies of revolution, the drag coefficient of a circular cylinder may be used, for which data are plentiful. However, for bodies with cross-sectional shapes other than circular, drag data are meager (e.g., see ref. 3). It is the purpose of this report to present drag coefficients over a fairly wide range of Reynolds numbers ($R = 10^4$ to 2×10^6) for a variety of cross sections. The measured drag coefficient for the circular cylinder in the subcritical Reynolds number range was lower than the generally accepted value. Eliminating the cause of this discrepancy, end leakage, would have complicated unduly the testing technique, and, hence, the leakage was allowed to remain.

SYMBOLS

b frontal width of cylinder

b_o frontal width of basic cylinder without rounded corners

c streamwise dimension of cylinder

c_o streamwise dimension of basic cylinder without rounded corners

c_d drag coefficient, $\frac{\text{drag per unit length}}{qb}$

f frequency of vortex discharge from one side of cylinder

M free-stream Mach number

q free-stream dynamic pressure

R Reynolds number based on c

r cross-sectional corner radius of cylinder

V free-stream velocity

$\frac{b_o}{c_o}$ cross-sectional fineness ratio of basic cylinder

$\frac{r}{b_o}$ cross-sectional corner-radius ratio of cylinder

$\frac{fb}{V}$ Strouhal number

CORRECTIONS

The drag coefficients and Reynolds numbers have been corrected for the effects of the wind-tunnel walls by the method of reference 4. The corrections used were as follows:

$$c_d = c_d' - \frac{[2 - (M')^2][1 + 0.4(M')^2]}{1 - (M')^2}\left(\frac{b}{40}\right)\left(c_d'\right)^2$$

$$R = R' + \frac{[1 - 0.7(M')^2][1 + 0.4(M')^2]}{1 - (M')^2}\left(\frac{b}{40}\right) c_d' R'$$

The primed values are the uncorrected values.

No correction has been made for the effect of spanwise flow due to leakage where the cylinders passed through the tunnel walls or due to the boundary layers on the walls of the wind tunnel.

MODEL DESCRIPTION AND APPARATUS

To obtain data over the desired Reynolds number range it was necessary to construct cylinders of three different sizes for each cross-sectional shape. Sketches of the cross-sectional shapes and the characteristic dimensions are presented in table I. The size of each cylinder is designated by a nominal dimension (either 1, 4, or 12 inches) which corresponds to a dimension of the basic cross-sectional shape. For the circles and ellipses the nominal dimension is the diameter or major axis. For the cylinders with basic cross sections composed of straight lines, the nominal dimension is the length of the longest side, except for the isosceles triangle for which the length of the base was taken as the nominal dimension and the diamond for which the longest diagonal was taken as the nominal dimension.

The corners of all the cylinders were rounded so that the cylinders of different sizes had comparable corner-radius ratios (r/b_o). The three radius ratios for the 12-inch cylinders were obtained by successively rounding the corners with radii from 1/4 inch to a maximum of 4 inches. The corners of the 4-inch cylinders were rounded to correspond to only the smallest and largest radius ratios of the 12-inch cylinders. Only the smallest radius ratio was tested on the 1-inch cylinders.

The 12- and 4-inch cylinders were constructed of pine and were lacquered to produce highly polished surfaces. All the 12- and 4-inch cylinders were mounted vertically in the test section of the wind tunnel (fig. 1). The clearances or gaps between the ends of the cylinders and the wind-tunnel walls were of the order of 1/16 inch. Force measurements were made by means of the wind-tunnel balance system with these gaps unsealed.

The 1-inch cylinders were constructed of metal with smooth ground surfaces. These models were mounted between end plates (fig. 2) with gaps between the end plates and the model of about 1/32 inch. The forces were measured by means of a strain-gage balance (fig. 3).

The accuracy of each cylinder was checked at several spanwise locations by means of templates. A visual check showed that both the contour accuracy and straightness of the cylinders were satisfactory.

Measurements of the frequency of the pressure fluctuations were made in the wake for a number of the 12-inch cylinders by means of a pressure-sensitive cell mounted in the tip of a probe. The cell was brought to within 12 to 18 inches of the downstream surfaces of these cylinders and

then located so that the pressure fluctuations produced by the vortices shed from one side of the cylinders could be measured. In a few cases, simultaneous measurements were made on both sides of the wake with a pair of cells.

The tests were made in the Ames 7- by 10-foot wind tunnel. The variation of the average free-stream velocity and Mach number with Reynolds number is shown in figure 4.

RESULTS

The variations of drag coefficient with Reynolds number for the various cylinders tested are presented in figures 5 to 14. The data for the circular cylinder are presented in figure 5; the fineness ratio 1:2 and 2:1 ellipses in figure 6; the fineness ratio 1:2, 1:1, and 2:1 rectangular cylinders in figures 7, 8, and 9; the fineness ratio 1:2, 1:1, and 2:1 diamond cylinders in figures 10, 11, and 12; the isosceles triangular cylinders with the apex forward and with the base forward in figures 13 and 14. Also shown in these figures is the variation of Strouhal number with Reynolds number for those cases where measurements of the pressure fluctuations in the wake were made.

Comparison of the values of the drag coefficients for a circular cylinder from references 5 and 6 with the data of the present investigation (fig. 5) indicates sizable differences for subcritical Reynolds numbers ($R = 1.3 \times 10^4$ to 2.5×10^5). The values of the drag coefficient obtained for the 4- and 12-inch circular cylinders are approximately 1.0, as compared to 1.2 obtained in the previously cited investigations. This difference in the drag coefficient was due to the flow of air through the gaps in the tunnel walls at the ends of the model. Pressure distributions (not presented) measured at the midspan of the cylinders with the gaps between the wind-tunnel walls and the cylinder sealed and unsealed indicated this to be true. The effect of sealing the gaps was to decrease the pressure on the lee side of the cylinder. This effect is assumed to be the result of preventing the flow of air of approximately free-stream static pressure into the separated region on the lee side of the cylinder. It was not possible to evaluate the effects of the end leakage on the drag coefficient of the circular cylinder at supercritical Reynolds numbers because the drag coefficients could not be calculated from the pressure distributions with sufficient accuracy. However, comparison with the data of references 5 and 6 indicates that the critical Reynolds number ranges are in good agreement, and at supercritical Reynolds numbers of 5×10^5 and 6×10^5, the agreement of the drag coefficients is reasonable.

Some influence of end leakage on the drag measurements for all the other cylinders may have been present also. It is felt that the data are sufficiently accurate to indicate, at least qualitatively, the changes in

drag of the various shapes (ellipses, rectangles, diamonds, and triangles) with corner radius ratio and fineness ratio.

Table I presents values of the drag coefficient at Reynolds numbers of 10^5 (except where the lowest test Reynolds number was about 2×10^5) for the various shapes tested. Examination of these data indicate that the drag coefficient either remained essentially constant or decreased with an increase of the corner radius ratio and that, in general, the drag coefficient decreased with increasing fineness ratio.

Although the Strouhal number data were meager, comparison of the data of figures 5 to 14 indicates that at subcritical Reynolds numbers the Strouhal numbers for all the shapes were close to 0.2.

At supercritical Reynolds numbers the Strouhal number data presented are for the predominant frequencies encountered, with the exception of the fineness ratio 2:1 rectangle where the disturbances in the wake were periodic and had a value of about 0.4.

Ames Aeronautical Laboratory
National Advisory Committee for Aeronautics
Moffett Field, Calif., Aug. 25, 1953

REFERENCES

1. Allen, H. Julian, and Perkins, Edward W.: A Study of Effects of Viscosity on Flow Over Slender Inclined Bodies of Revolution. NACA Rep. 1048, 1951.

2. Van Dyke, Milton D.: First-Order and Second-Order Theory of Supersonic Flow Past Bodies of Revolution. Jour. Aero. Sci., vol. 18, no. 3, Mar. 1951, pp. 161-179.

3. Lindsey, Walter Frank: Drag of Cylinders of Simple Shapes. NACA Rep. 619, 1938.

4. Allen, H. Julian, and Vincenti, Walter G.: Wall Interference in a Two-Dimensional-Flow Wind Tunnel, with Consideration of the Effect of Compressibility. NACA Rep. 782, 1944.

5. Stack, John: Compressibility Effects in Aeronautical Engineering. NACA ACR, 1941.

6. Bursnall, William J., and Loftin, Laurence K., Jr.: Experimental Investigation of the Pressure Distribution About a Yawed Circular Cylinder in the Critical Reynolds Number Range. NACA TN 2463, 1951.

7. Relf, E. F., and Simmons, L. F. G.: The Frequency of the Eddies Generated by the Motion of Circular Cylinders Through a Fluid. R. & M. 917, British A.R.C., 1924.

TABLE I.- GEOMETRIC AND DRAG CHARACTERISTICS OF THE MODELS
[All dimensions in inches]

Flow direction →	Fineness ratio, (c_o/b_o)	Corner-radius ratio, (r/b_o)	Nominal size	b_o	b	c_o	c	r	c_d at $R=10^5$
	1:1	0.50	12	12.00	12.00	12.00	12.00	6.00	
	1:1	.50	4	4.00	4.00	4.00	4.00	2.00	1.00
	1:1	.50	1	1.00	1.00	1.00	1.00	.50	
	1:2	- - -	12	12.00	12.00	6.00	6.00	- - -	
	1:2	- - -	4	4.00	4.00	2.00	2.00	- - -	1.6
	1:2	- - -	1	1.00	1.00	.50	.50	- - -	
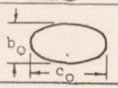	2:1	- - -	12	6.00	6.00	12.00	12.00	- - -	
	2:1	- - -	4	2.00	2.00	4.00	4.00	- - -	.6
	2:1	- - -	1	.50	.50	1.00	1.00	- - -	
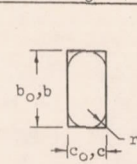	1:2	.021	12	12.00	12.00	6.00	6.00	.25	
	1:2	.021	4	4.00	4.00	2.00	2.00	.08	2.2
	1:2	.021	1	1.00	1.00	.50	.50	.021	
	1:2	.083	12	12.00	12.00	6.00	6.00	1.00	1.9
	1:2	.250	12	12.00	12.00	6.00	6.00	3.00	1.6
	1:2	.250	4	4.00	4.00	2.00	2.00	1.00	
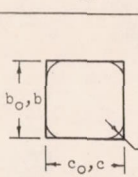	1:1	.021	12	12.00	12.00	12.00	12.00	.25	
	1:1	.021	4	4.00	4.00	4.00	4.00	.08	2.0
	1:1	.021	1	1.00	1.00	1.00	1.00	.021	
	1:1	.167	12	12.00	12.00	12.00	12.00	2.00	1.2[a]
	1:1	.333	12	12.00	12:00	12.00	12.00	4.00	1.0
	1:1	.333	1	1.00	1.00	1.00	1.00	.33	
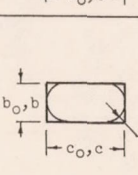	2:1	.042	12	6.00	6.00	12.00	12.00	.25	
	2:1	.042	4	2.00	2.00	4.00	4.00	.08	1.4
	2:1	.042	1	.50	.50	1.00	1.00	.021	
	2:1	.167	12	6.00	6.00	12.00	12.00	1.00	.7[a]
	2:1	.500	12	6.00	6.00	12.00	12.00	3.00	.4
	2:1	.500	4	2.00	2.00	4.00	4.00	1.00	

Flow direction →	Fineness ratio, (c_o/b_o)	Corner-radius ratio, (r/b_o)	Nominal size	b_o	b	c_o	c	r	c_d at $R=10^5$
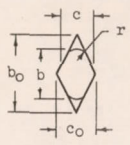	1:2	0.021	12	12.00	11.38	6.00	5.94	0.25	
	1:2	.021	4	4.00	3.77	2.00	1.98	.08	1.8
	1:2	.021	1	1.00	.95	.50	.49	.021	
	1:2	.083	12	12.00	9.53	6.00	5.76	1.00	1.7
	1:2	.167	12	12.00	7.05	6.00	5.53	2.00	1.7
	1:2	.167	4	4.00	2.35	2.00	1.84	.67	
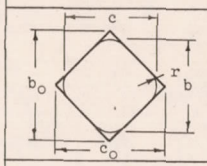	1:1	.015	12	16.97	16.76	16.76	16.80	.25	
	1:1	.015	4	5.66	5.59	5.66	5.59	.08	1.5
	1:1	.015	1	1.41	1.39	1.41	1.39	.021	
	1:1	.118	12	16.97	15.31	16.97	15.31	2.00	1.5[a]
	1:1	.235	12	16.97	13.66	16.97	13.66	4.00	1.5
	1:1	.235	4	5.66	4.55	5.66	4.55	1.33	
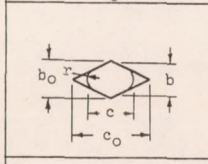	2:1	.042	12	6.00	5.94	12.00	11.42	.25	
	2:1	.042	4	2.00	1.98	4.00	3.88	.08	1.1
	2:1	.042	1	.50	.49	1.00	.96	.02	
	2:1	.167	12	6.00	5.76	12.00	9.50	1.00	1.1[a]
	2:1	.333	12	6.00	5.53	12.00	7.05	2.00	1.1
	2:1	.333	4	2.00	1.84	4.00	2.35	.67	
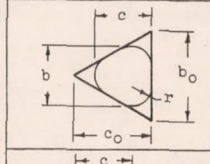	1:1	.021	12	12.00	11.69	12.00	11.69	.25	
	1:1	.021	4	4.00	3.90	4.00	3.90	.08	1.2
	1:1	.021	1	1.00	.98	1.00	.98	.021	
	1:1	.083	12	12.00	10.77	12.00	10.77	1.00	1.3[a]
	1:1	.250	12	12.00	8.29	12.00	8.29	3.00	1.1
	1:1	.250	4	4.00	2.78	4.00	2.76	1.00	
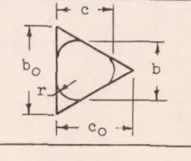	1:1	.021	12	12.00	11.69	12.00	11.69	.25	
	1:1	.021	4	4.00	3.90	4.00	3.90	.08	2.0
	1:1	.021	1	1.00	.98	1.00	.98	.021	
	1:1	.083	12	12.00	10.77	12.00	10.77	1.00	1.9[a]
	1:1	.250	12	12.00	8.29	12.00	8.29	3.00	1.3
	1:1	.250	4	4.00	2.76	4.00	2.76	1.00	

[a] $R = 2 \times 10^5$

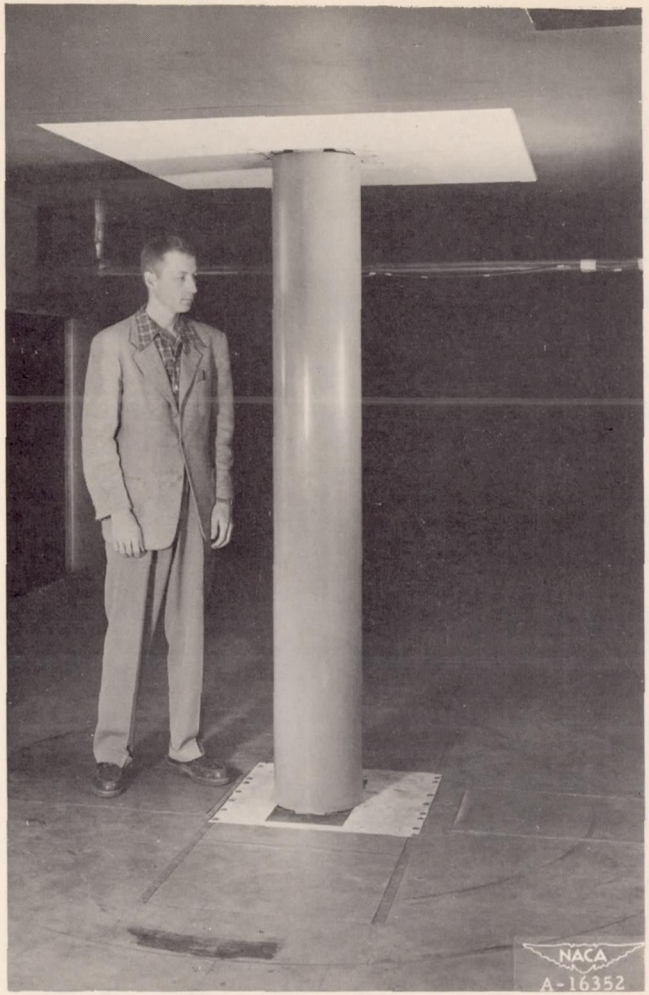

(a) 12-inch circular cylinder.

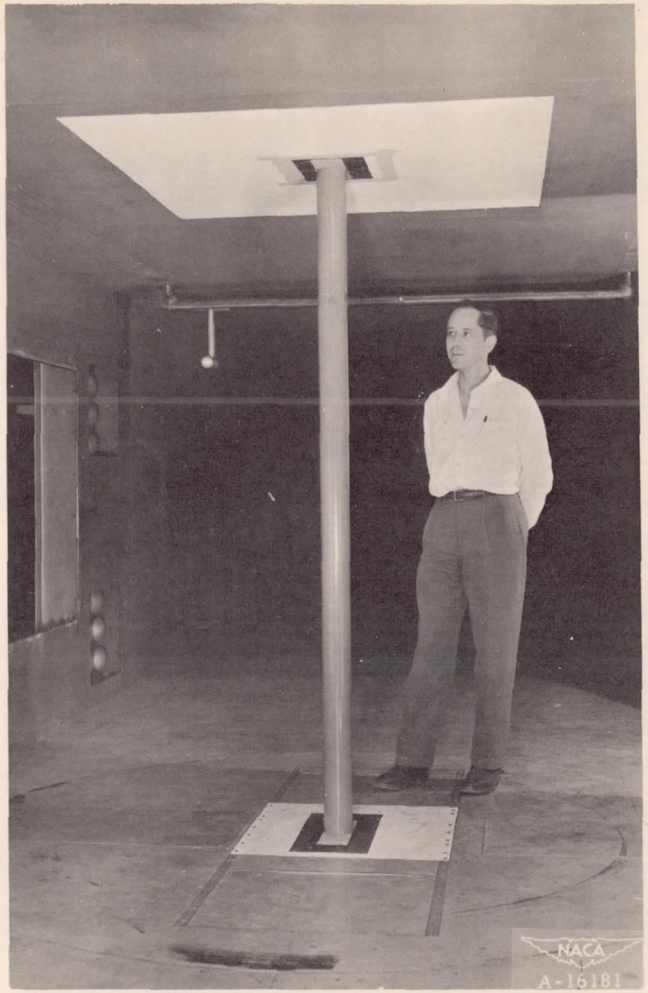

(b) 4-inch circular cylinder.

Figure 1.- Method of mounting 12-inch and 4-inch cylinders in the wind tunnel.

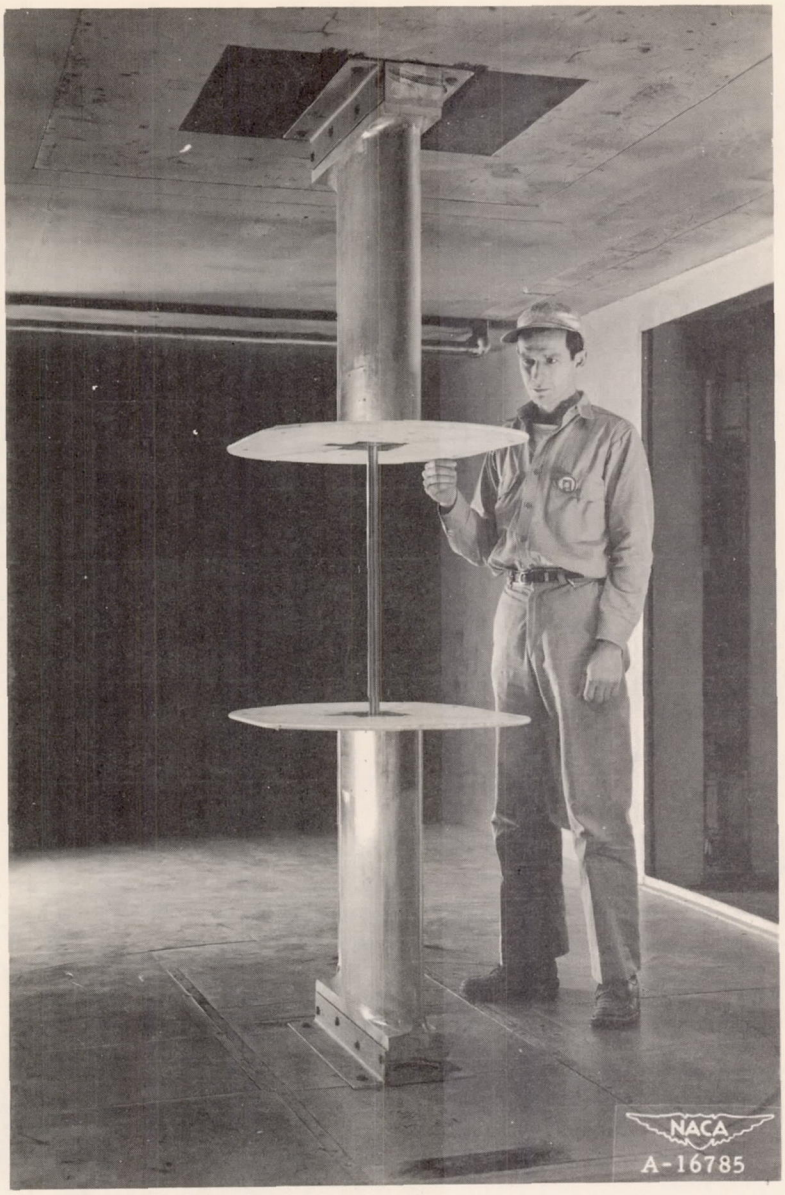

Figure 2.- Method of mounting 1-inch cylinders between end plates in the wind tunnel.

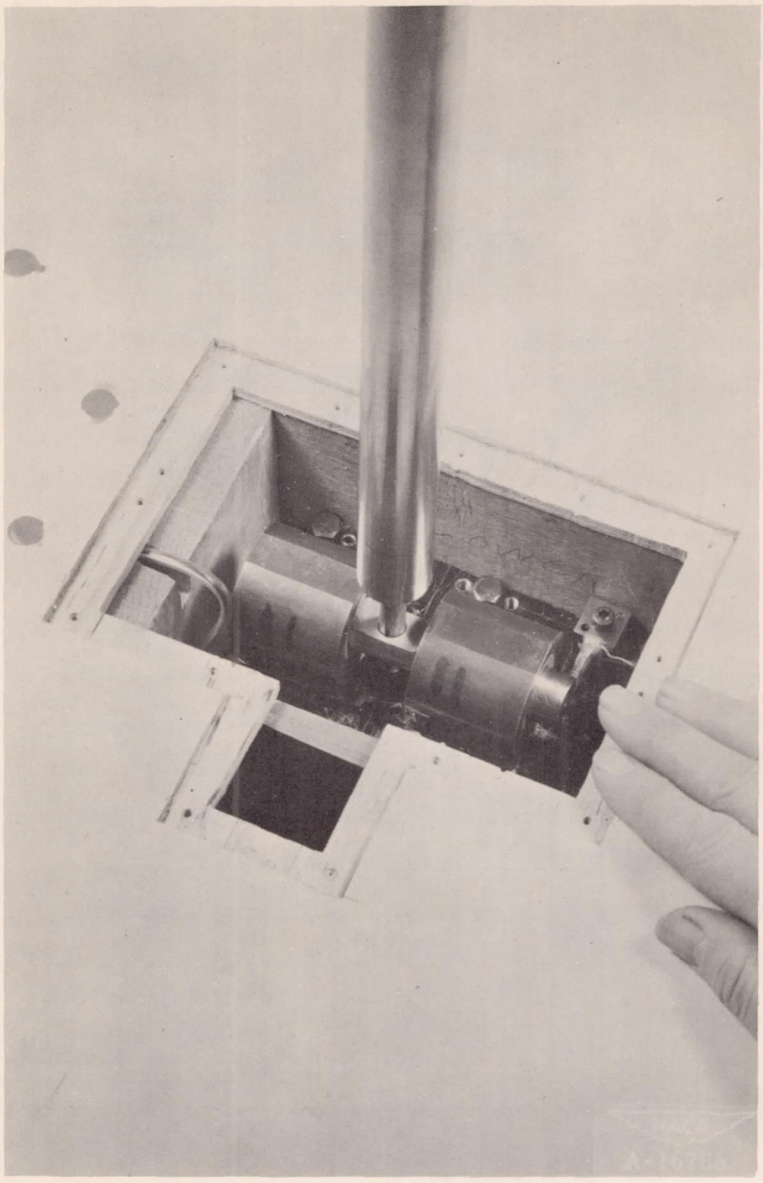

Figure 3.- The strain-gage balance for the 1-inch cylinders.

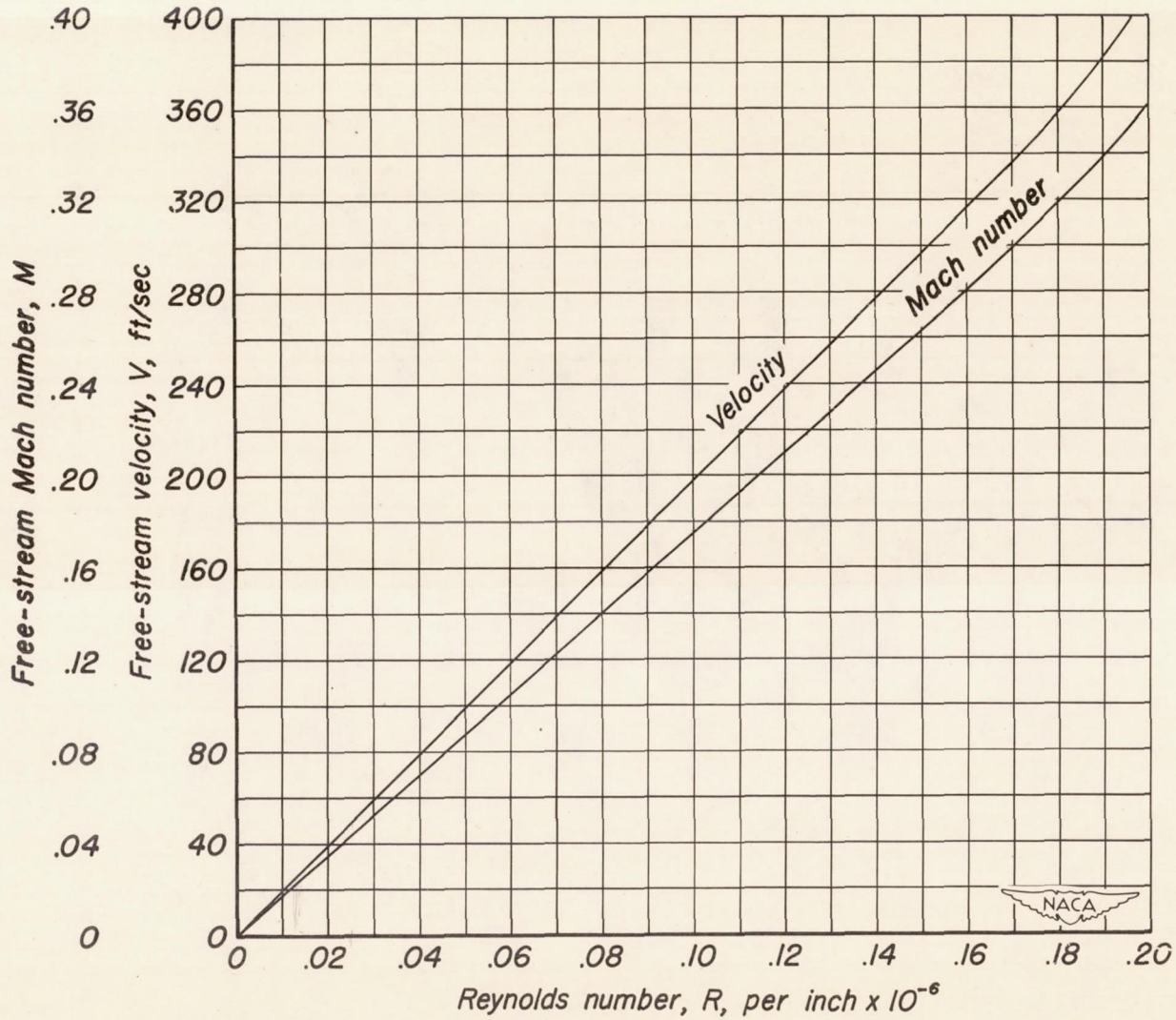

Figure 4.—Variation of average free-stream velocity and Mach number with Reynolds number.

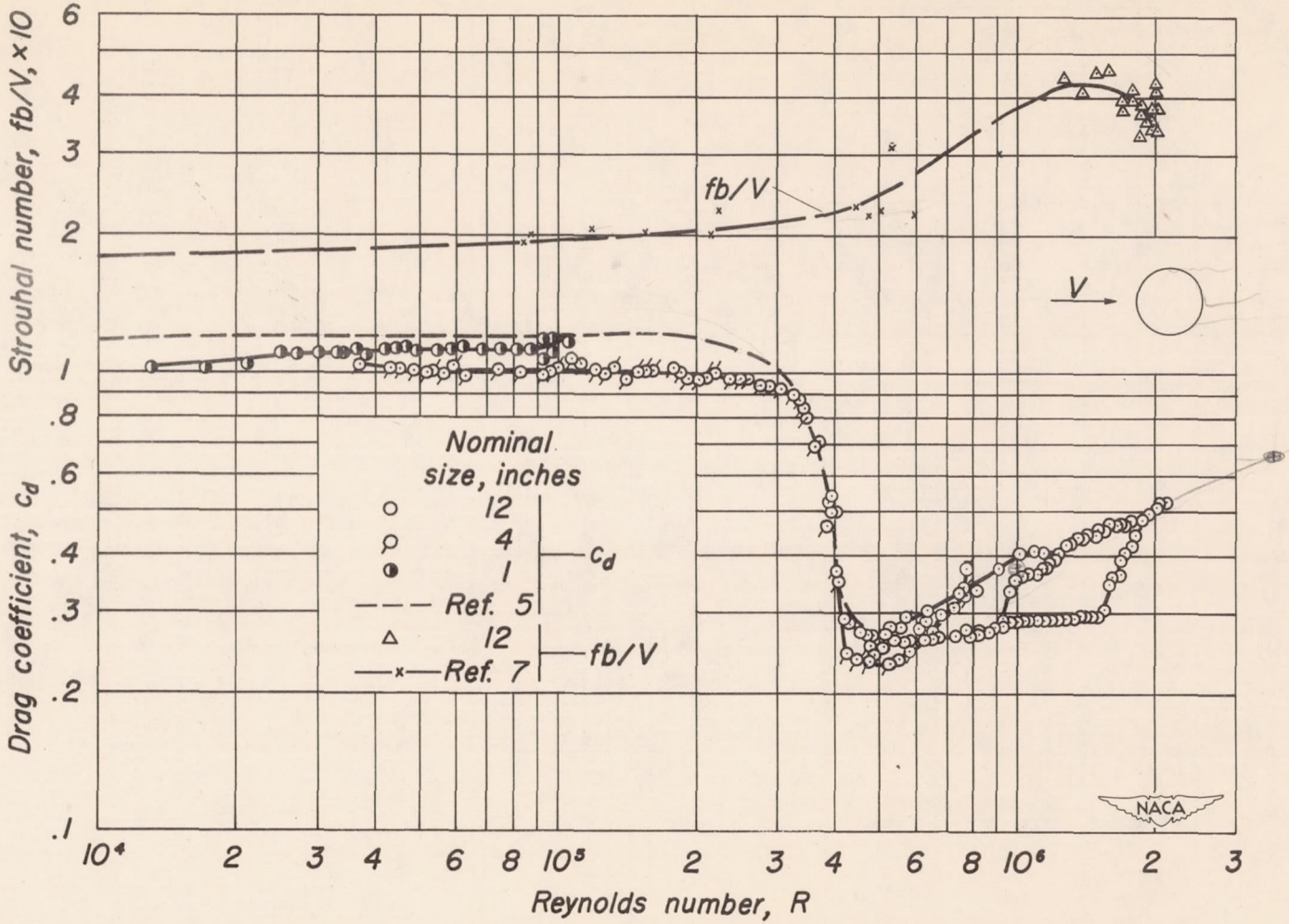

Figure 5.–Variation of drag coefficient and Strouhal number with Reynolds number for the circular cylinders.

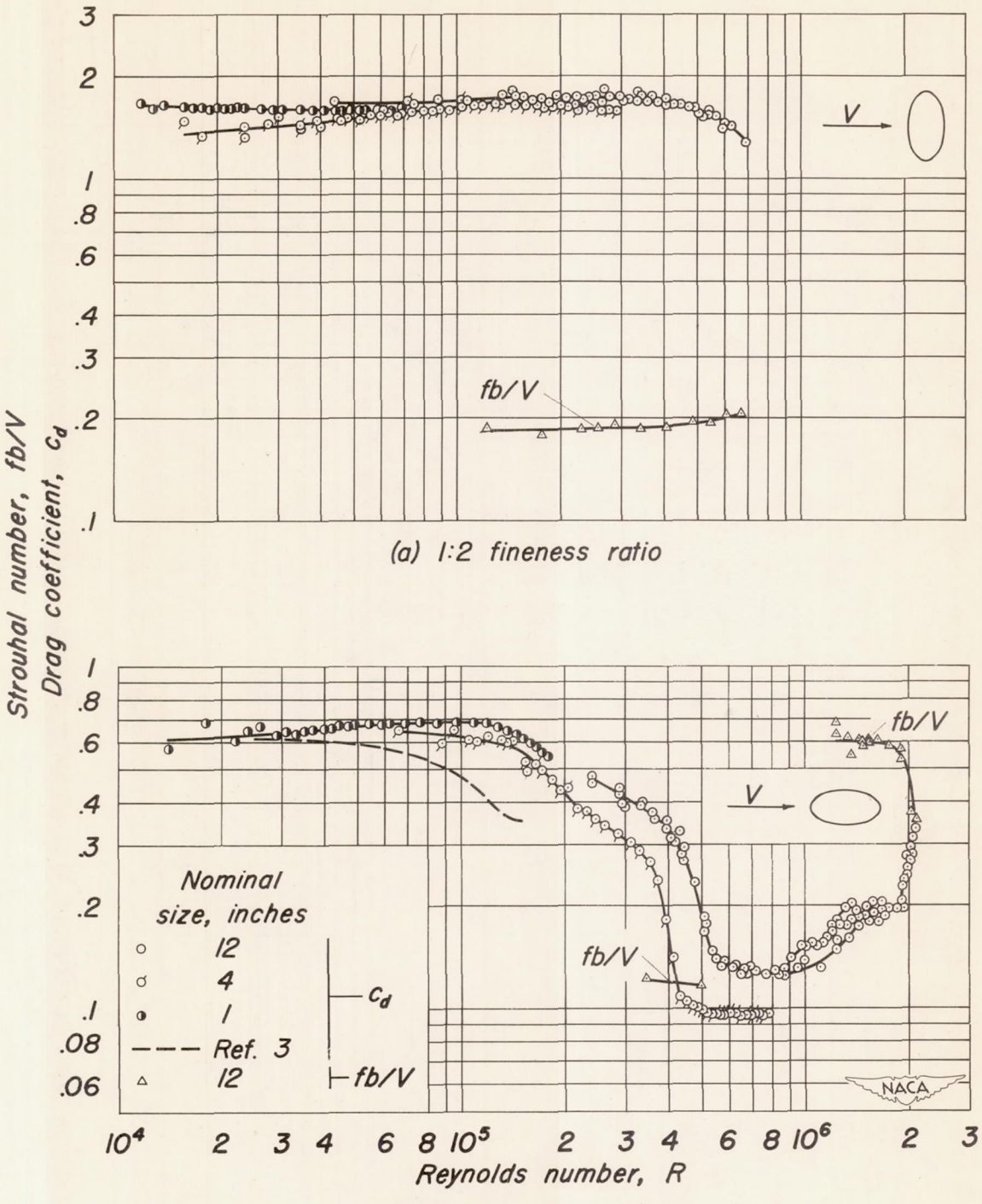

Figure 6.—Variation of drag coefficient and Strouhal number with Reynolds number for the elliptic cylinders.

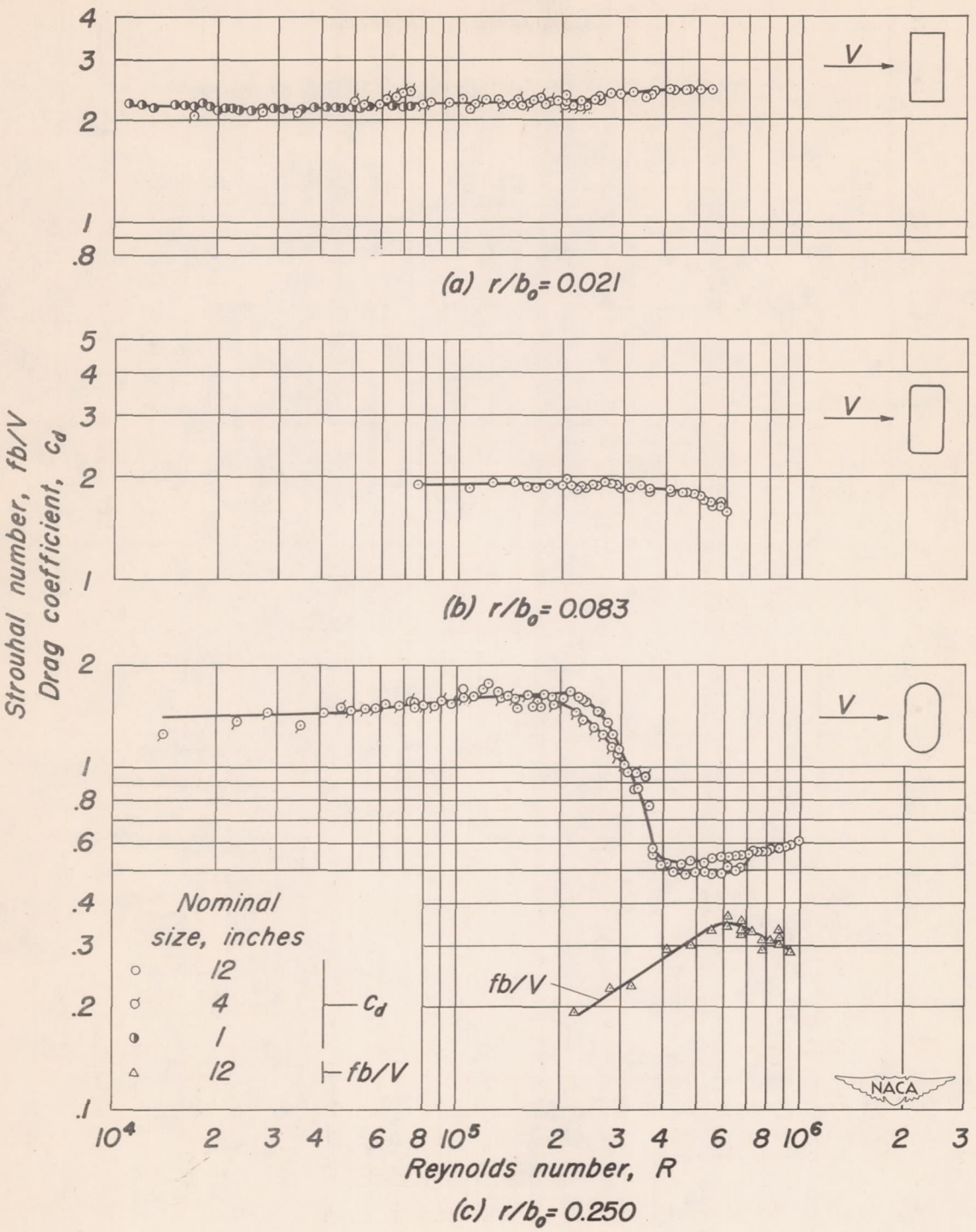

Figure 7.—Variation of drag coefficient and Strouhal number with Reynolds number for the 1:2 fineness ratio rectangular cylinders.

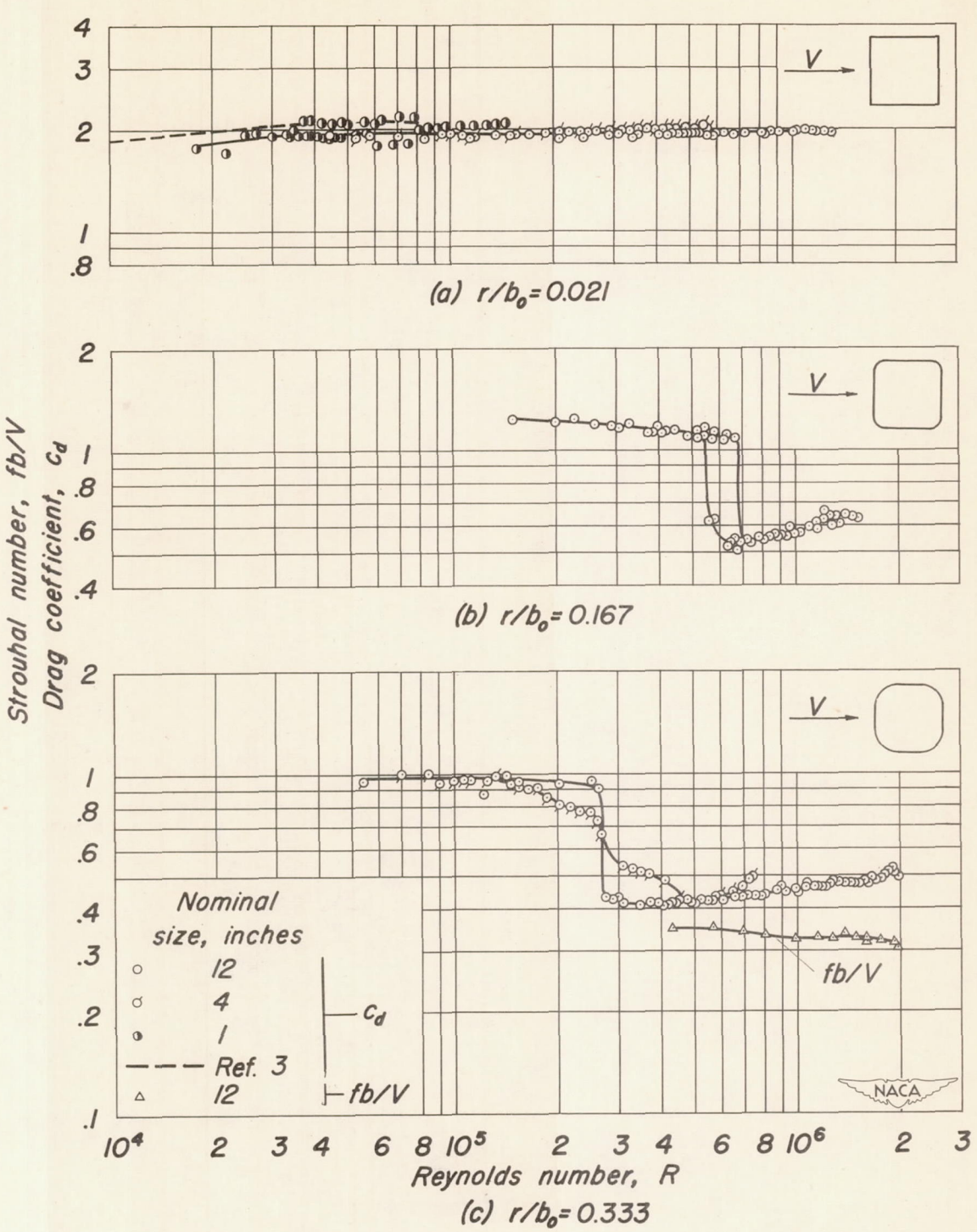

Figure 8.—Variation of drag coefficient and Strouhal number with Reynolds number for the 1:1 fineness ratio rectangular cylinders.

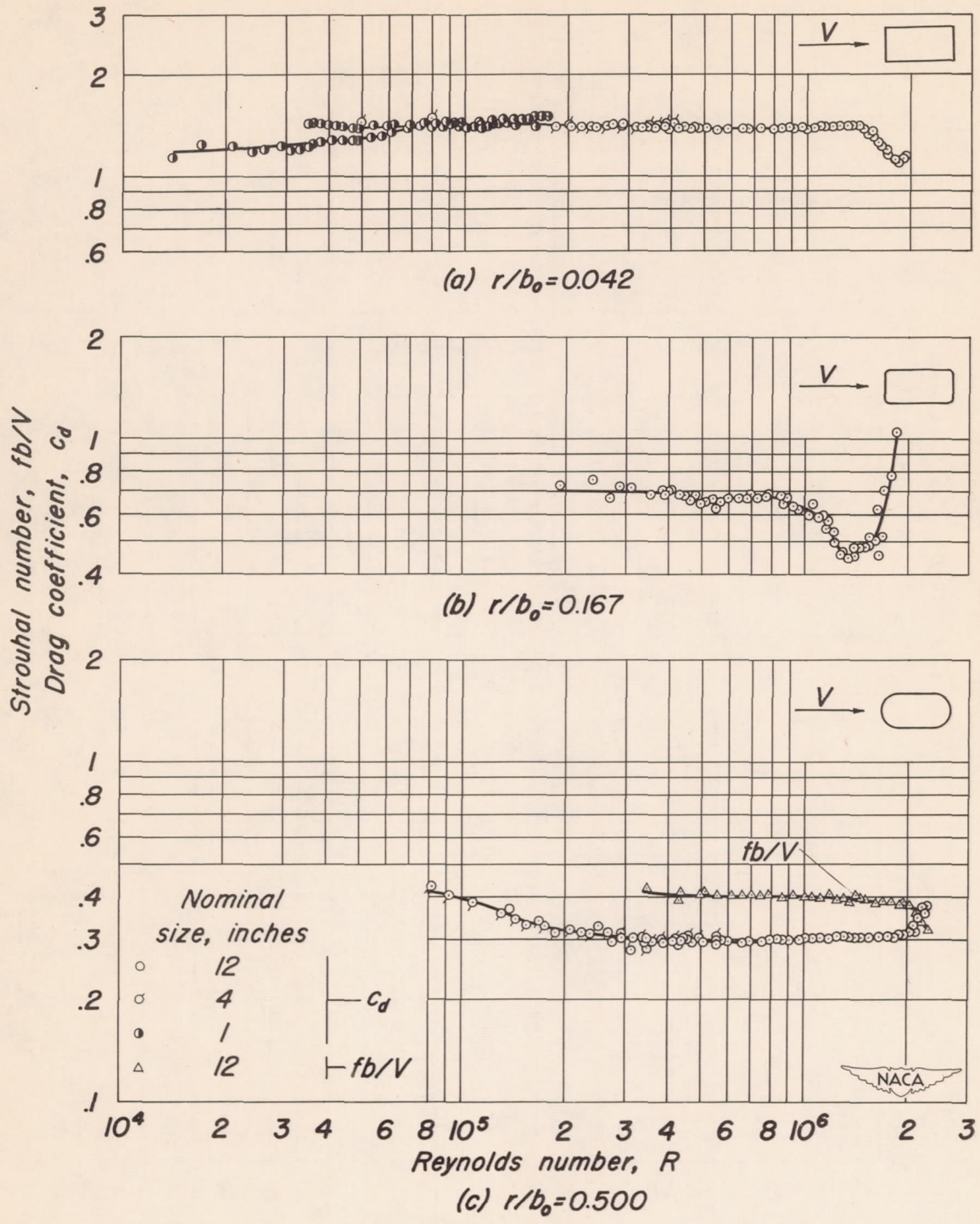

Figure 9.—Variation of drag coefficient and Strouhal number with Reynolds number for the 2:1 fineness ratio rectangular cylinders.

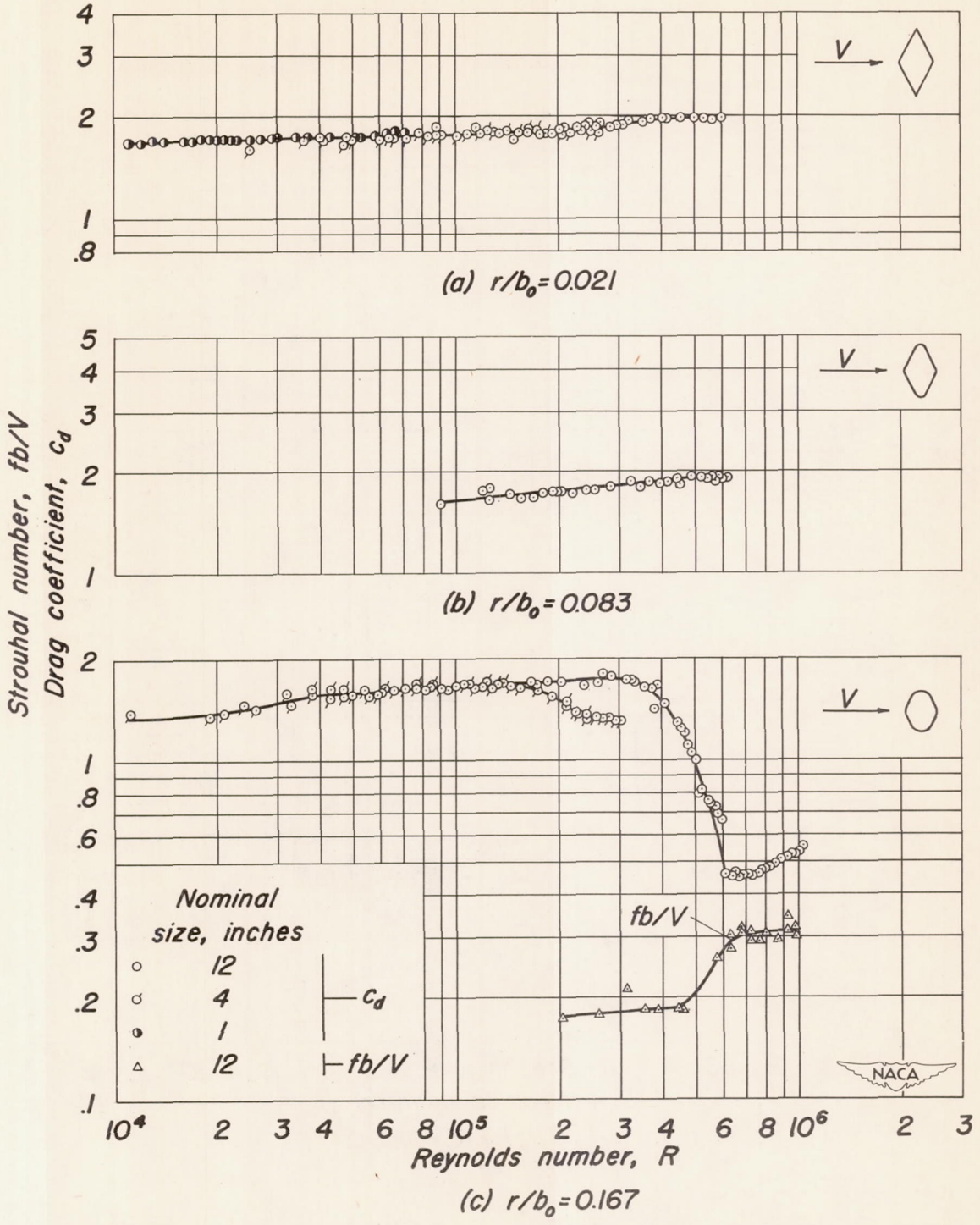

Figure 10.—Variation of drag coefficient and Strouhal number with Reynolds number for the 1:2 fineness ratio diamond cylinders.

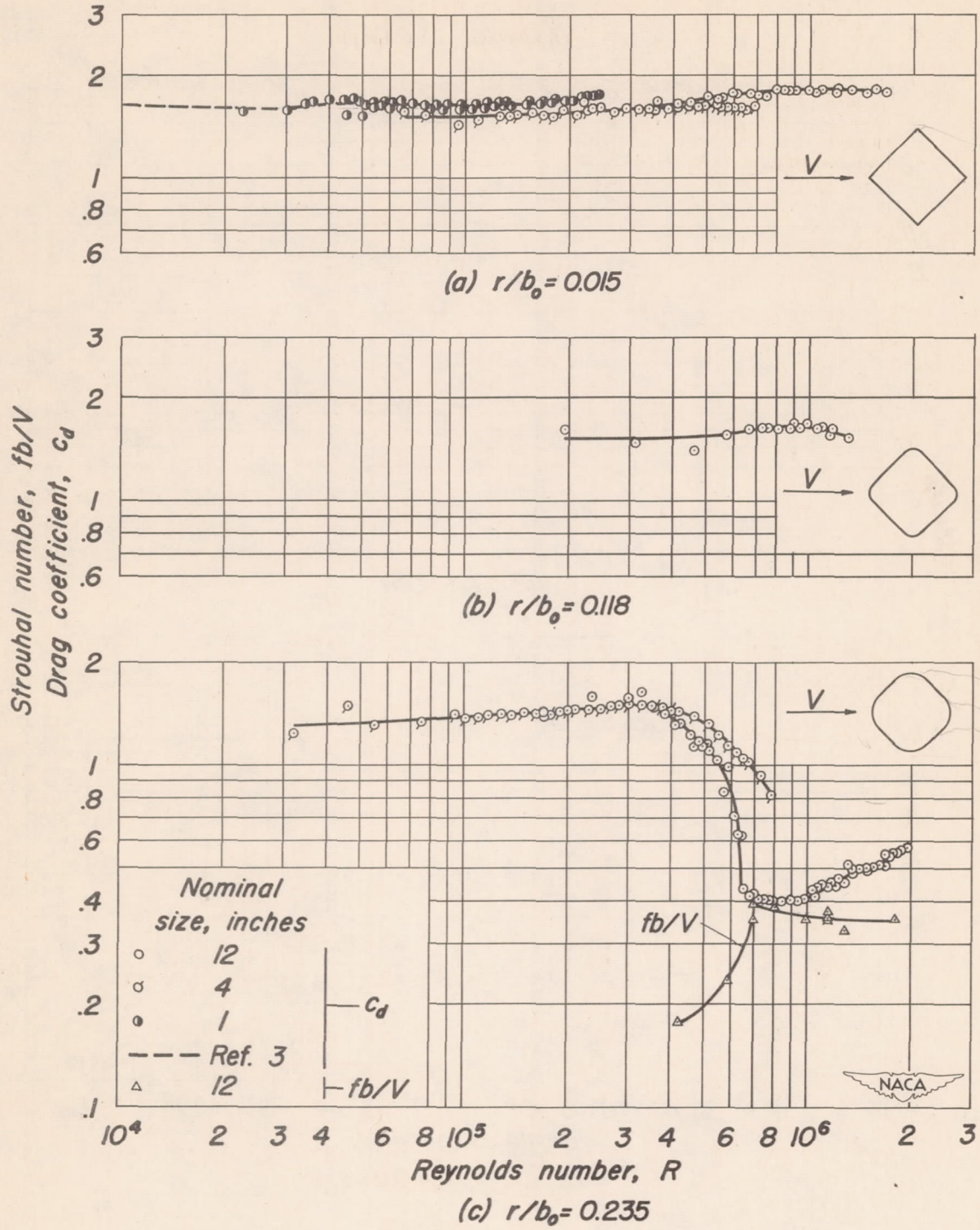

Figure 11.—Variation of drag coefficient and Strouhal number with Reynolds number for the 1:1 fineness ratio diamond cylinders.

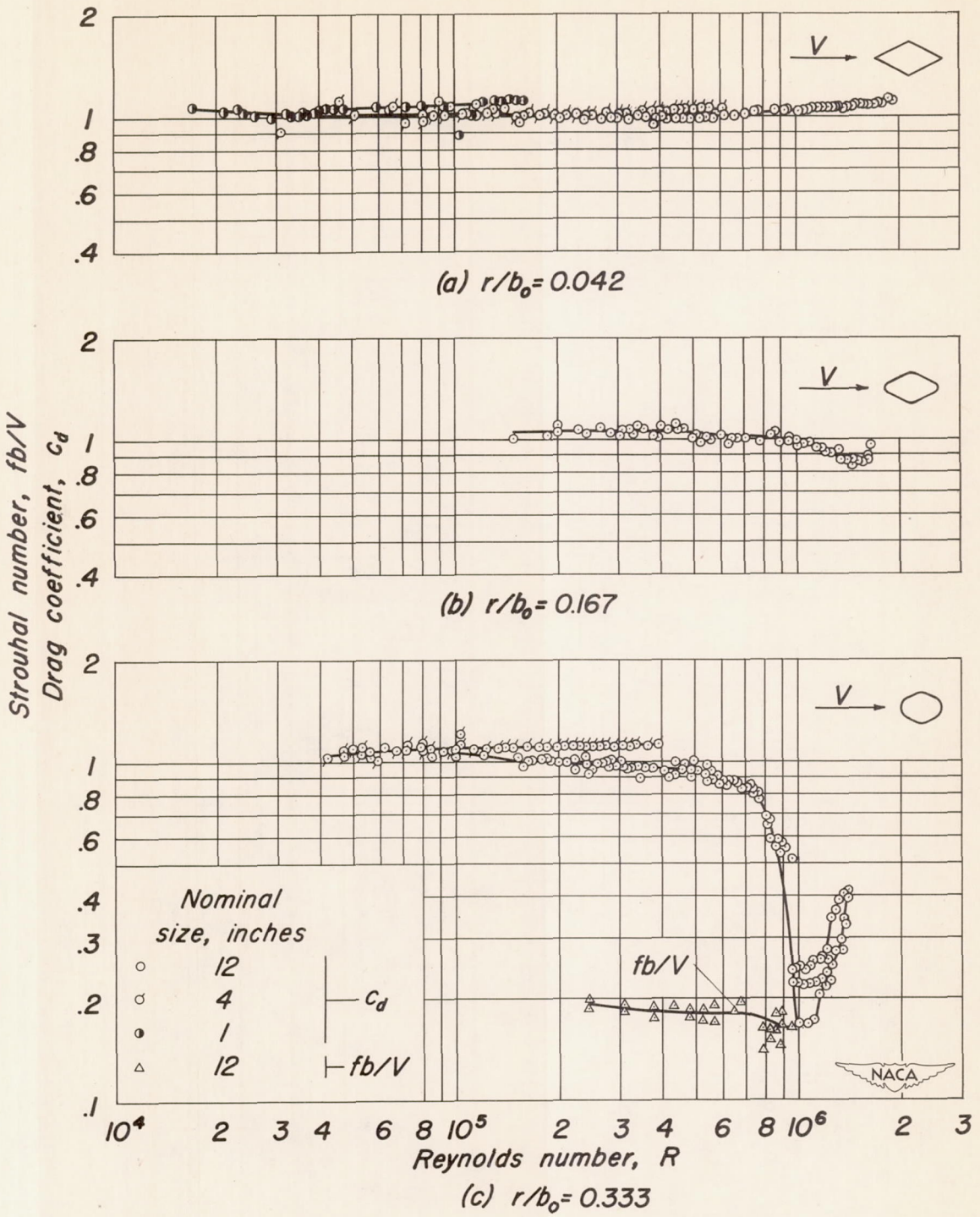

Figure 12.—Variation of drag coefficient and Strouhal number with Reynolds number for the 2:1 fineness ratio diamond cylinders.

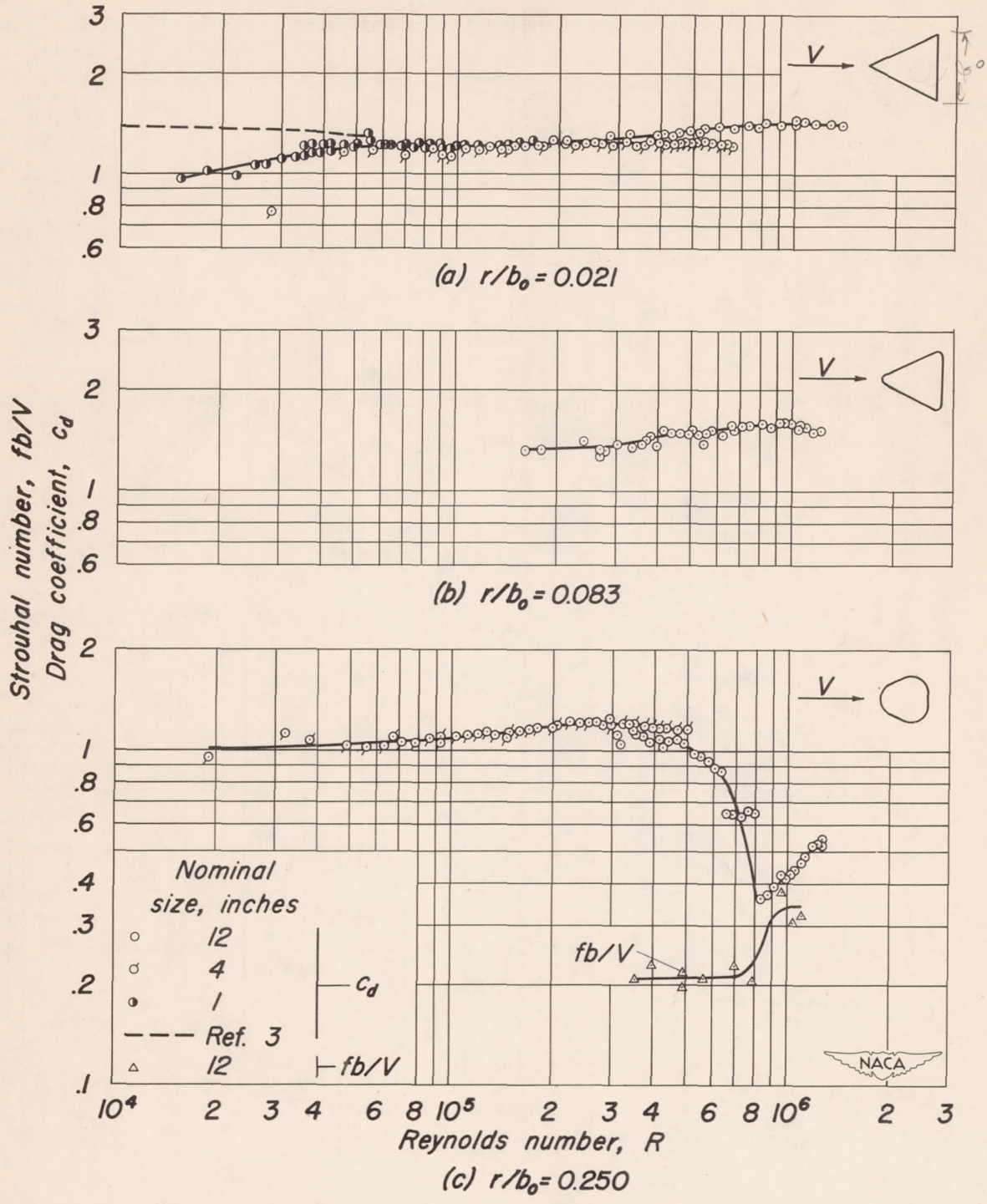

Figure 13.—Variation of drag coefficient and Strouhal number with Reynolds number for the isosceles triangular cylinders with apex forward.

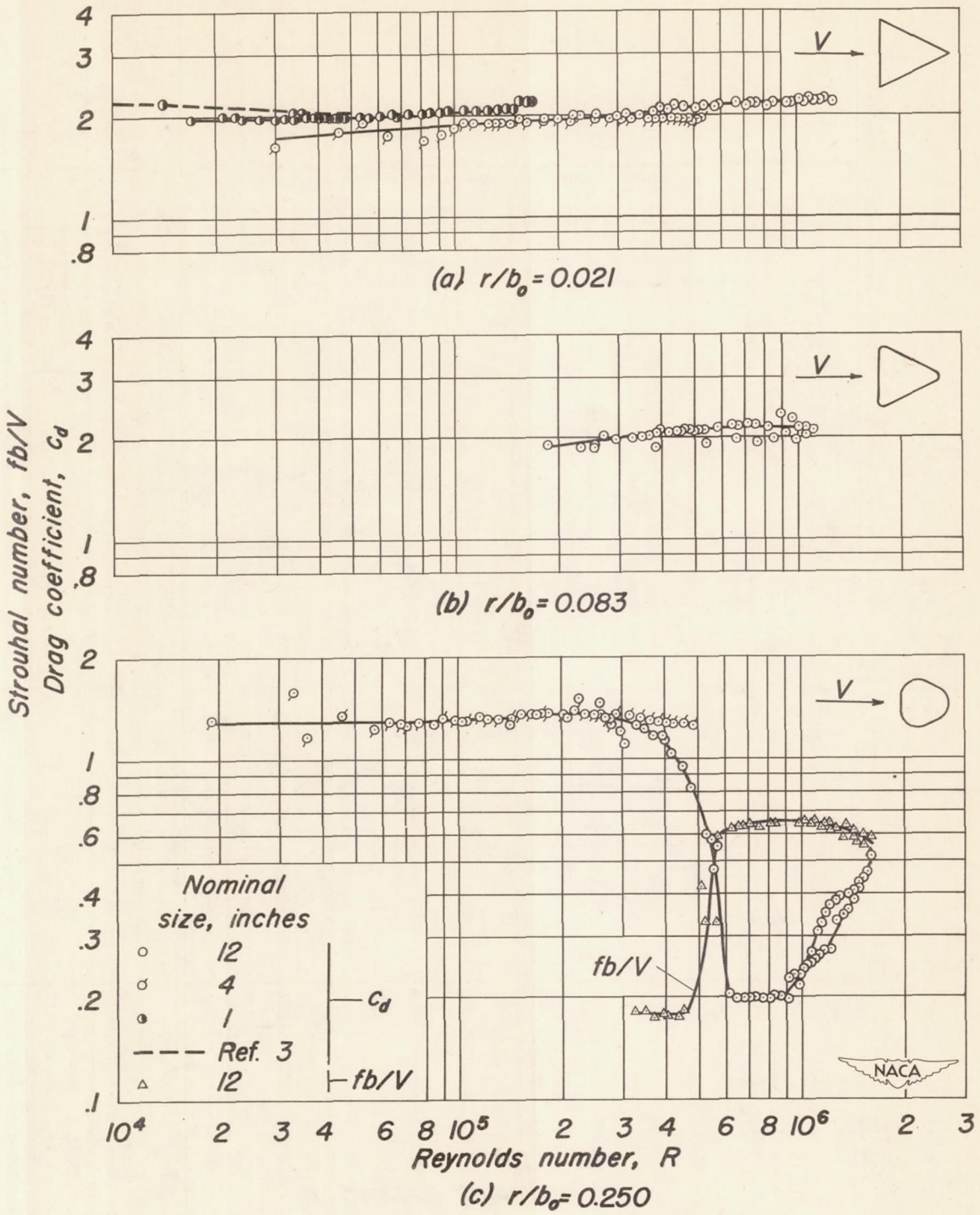

Figure 14.—Variation of drag coefficient and Strouhal number with Reynolds number for the isosceles triangular cylinders with base forward.